引用格式：HUANG Jiaxu，LI Jun，QIU Pei，et al. Laser-induced Two-dimensional Surface Nanopatterning on Film Materials (Invited)[J]. Acta Photonica Sinica，2023，52(7)：0752302
黄佳旭，李峻，邱佩，等．激光诱导薄膜材料二维图案化纳米加工技术(特邀)[J]．光子学报，2023，52(7)：0752302
※封底论文※

激光诱导薄膜材料二维图案化纳米加工技术(特邀)

黄佳旭，李峻，邱佩，徐少林
(南方科技大学 机械与能源工程系，深圳 518055)

摘　要：激光诱导周期性表面结构(Laser-Induced Periodic Surface Structures，LIPSS)是一种在激光辐照下自发生成的超衍射极限结构，但其结构类型较为单一。提出了一种新型的二维图案化激光纳米加工方法，通过同时利用激光诱导的热效应及表面等离激元干涉，在正交的两个方向上分别形成褶皱和LIPSS两种周期性结构。这种方法仅通过单步辐照就能在薄膜材料表面生成二维褶皱LIPSS，从而丰富LIPSS的结构类型。同时，通过调整加工材料的膜厚或基底，以及改变入射激光波长或角度，可以分别调制二维纳米结构在两个正交方向上的周期。此外，通过激光偏振也可以调控该结构的取向。该方法能够进一步拓宽基于LIPSS的可加工表面纳米结构的种类及应用。

关键词：超快激光；激光诱导周期性表面结构；激光诱导褶皱；薄膜材料；二维纳米结构；飞秒激光
中图分类号：TN249；TN241　　**文献标识码**：A　　**doi**：10.3788/gzxb20235207.0752302

0　引言

亚波长尺度周期性表面结构的制备技术对于光学、化学、材料和能源等领域的研究具有重要意义。近年来，激光诱导周期性表面结构(Laser-Induced Periodic Surface Structures，LIPSS)被广泛报导，其是一种在激光辐照下自发诱导形成的超衍射极限结构[1-3]。相比于传统的制备方法，基于LIPSS的表面结构加工技术具备制备效率高、材料选择性低、环境宽容度高、加工路径自由可控和可突破衍射极限等优势。尽管该技术已经被验证可以在极短时间内实现晶圆级面积内亚波长结构的高效均匀制备[4-7]，但由于其表面周期性能量沉积(通常是入射光与激光激发表面等离激元波(Surface Plasmon Polaritons，SPPs)的干涉)引起结构生成的机制[8]，LIPSS通常是一维的光栅结构。通过对激光进行时空调制[9-12]、多次扫描[4,13-14]、诱导表面等离激元干涉[15]或引入另一效应(如Marangoni效应[16]、入射光干涉[17]等)等方式能有效实现二维亚波长结构的制备。

在薄膜材料领域，LIPSS加工技术展示了广泛的应用前景。这种技术可以在众多薄膜材料上实现不同类型亚波长尺度的周期性结构制备，从而改善薄膜材料的性能，尤其在光学应用方面表现突出[18-21]。然而，在薄膜系统中，LIPSS技术在加工适用性、稳定性以及能量沉积和热影响等方面的深入研究仍然较少。因此，进一步探讨LIPSS技术在薄膜材料表面结构加工方面的应用将为功能性表面结构器件的发展开辟新的可能性。

本文提出了一种针对薄膜材料的二维周期性结构的高效制备方法。该方法通过调控激光沉积表面的热累积过程引起材料热膨胀诱导褶皱形成，并结合表面等离激元的激发，在薄膜材料表面实现二维周期性结构的制备，具有制备成本低、制备过程简单、制备效率高等优点。

基金项目：深圳市科技项目 (Nos. JCYJ20220818100408019，JSGG20210802154007021，KQTD20170810110250357)
第一作者：黄佳旭，12231126@mail.sustech.edu.cn
通讯作者：徐少林，xusl@sustech.edu.cn
收稿日期：2023-03-29；**录用日期**：2023-06-09

1 实验与设备

本研究中使用的样品主要为沉积在硅基底上的锗锑碲($Ge_2Sb_2Te_5$,GST)薄膜,其制备方法为:分别用酒精和异丙醇对硅基底(N型掺杂,<100>晶向)进行超声清洗10 min;然后,通过磁控溅射(KYKY500CK-500ZF)在基底上蒸镀相应的膜层,包括在硅基底上分别蒸镀了20 nm、40 nm和50 nm厚度的GST薄膜,以及在熔融石英基底上蒸镀了50 nm厚度的GST薄膜。在随后的激光纳米图案化加工过程中,通过飞秒激光系统(Spectra-Physics)提供了脉冲宽度为300 fs,中心波长为520 nm,脉冲重复频率为100 kHz的激光脉冲,随后通过半波片和格兰棱镜结合调整激光能量,并通过半波片调制激光偏振角度,而后激光束依次通过一个柱面透镜(焦距f = 25 mm)和一个物镜透镜(0.1 NA,4倍)聚焦,最终获得长度为8 mm,宽度为7.78 μm的线形聚焦光斑。结合高精度位移平台(Newport XMS100-S)控制样品的运动,且在激光加工过程中始终保持样品的运动方向垂直于线形光斑长轴的方向。同时,本研究还通过添加一个辅助气源对样品持续吹气及时排除激光烧蚀碎屑。在激光加工完成后,再分别使用酒精和异丙醇对加工样品进行超声清洗10 min。最后通过扫描电子显微镜(SEM,Zeiss,Merlin)和原子力显微镜(AFM,Bruker,Dimension Edge)对激光加工的表面形貌进行表征测量。

2 实验结果与分析

2.1 二维褶皱LIPSS的形成机制

如图1(a)、(b)所示,当激光以特定的脉冲能量和沉积数量辐照至薄膜材料表面时,可以在单次扫描过程中生成周期性二维纳米结构,也就是二维褶皱LIPSS。其实现原理可以简单总结为垂直偏振方向的LIPSS生成和平行偏振方向热形变引起的材料褶皱生成,具体过程为:在激光辐照下,如图1(c)所示,在垂直偏振方向的表面等离激元激发并进一步与入射激光干涉,从而形成周期性能量沉积,导致材料的周期性烧蚀,形成LIPSS结构[14-15,22];在平行偏振方向,如图1(d)所示,激光连续辐照将引起热累积,从而导致材料发生膨胀形变,同时,由于薄膜(GST)与基底(硅)材料的弹性模量和泊松比不同,导致薄膜材料在激光连续辐照下生成周期性褶皱[23]。上述两者不同取向的光学和力学机制将使得薄膜在正交的两个方向同步生成周期性结构,从而在单次扫描辐照中实现二维周期性结构的高效制备。

研究中激光垂直辐照至材料表面所生成的LIPSS周期Λ在数值上等于激光激发的表面等离激元波长

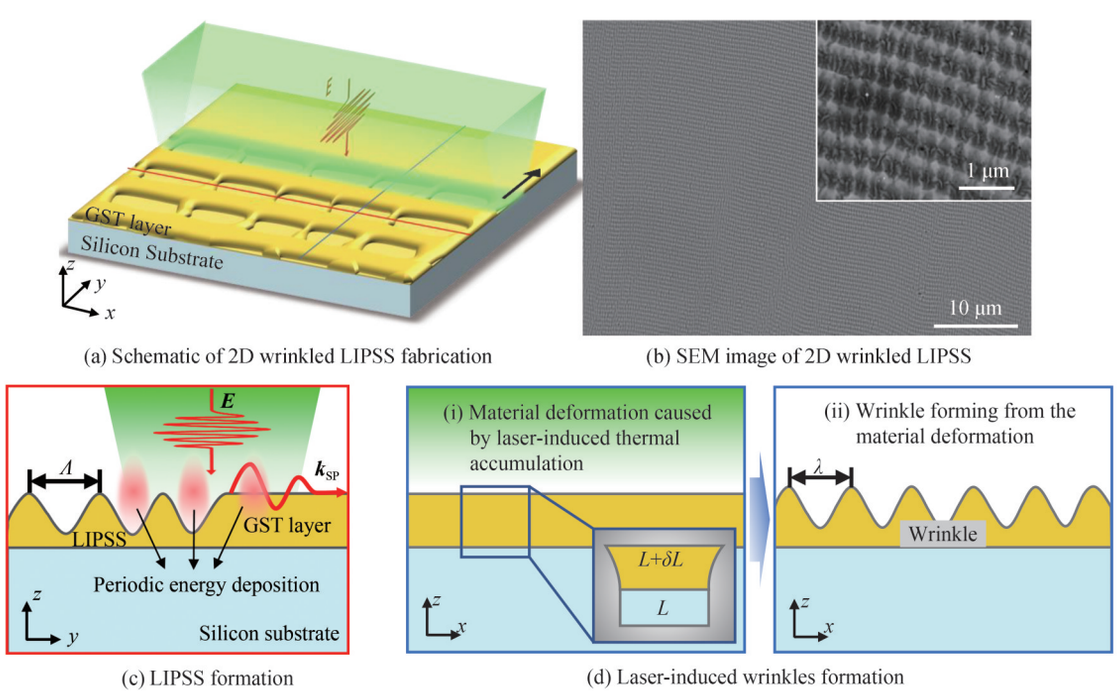

图1 激光加工二维褶皱LIPSS原理图及加工结果

Fig.1 Schematics and results of the fabrication of 2D wrinkled LIPSS

λ_{SPPs}（~410 nm），与前期工作研究一致[15,22]。同时，LIPSS周期Λ还可通过调控入射光波长和角度实现进一步调控[3]。如图1(d)所示，对于褶皱的形成过程可分为两步：1)激光辐照下薄膜材料被加热，引起薄膜材料的热膨胀形变，由于薄膜材料与基底材料的热膨胀系数不一致，导致薄膜材料的上下界面的形变程度不同；2)在形变过程中当材料所受应力超过其屈服强度，薄膜材料将发生塑性形变，最终获得周期性褶皱结构。这个过程产生的褶皱周期λ计算公式为[24-25]

$$\lambda = 2\pi\xi h\left(\frac{(1-\upsilon_s^{\,2})E_f}{(1-\upsilon_f^{\,2})E_s}\right)^{\frac{1}{3}} \tag{1}$$

式中，ξ为修正系数（通常取1），h为薄膜厚度，υ和E分别是材料的泊松比和杨氏模量，下标s和f表示基底材料和薄膜材料对应的力学参数，研究所使用材料力学参数如表1所示。

表1　GST、硅和石英的材料力学参数

Table 1　Mechanic parameters of GST, silicon and quartz

Materials	Poisson's ratio υ	Young's modulus E/GPa	Reference
GST	0.34	34	[26]
Si, <100>	0.28	129	[27]
SiO_2	0.17	73	

如图2(a)所示，在1 mm/s的扫描速度，100 kHz的脉冲重复频率和不同能量激光辐照下，硅基底上50 nm厚的GST薄膜形成的褶皱周期相对稳定（~270 nm），与式(1)所计算结果（~204 nm）存在一定差距。这是使用超快激光加工所导致的：由于超快激光加工过程是一连串的脉冲光源对材料进行辐照，引起材料的快速加热和冷却，从而使得激光诱导褶皱的形成过程相较于常规的加热或施加外力的过程更快地发生。因此，对式(1)加以修正，即加入修正系数ξ，其数值为拟合实验测量数据（选取周期稳定区域，即图中2(a)中脉冲能量在4.29~5.86 μJ的数据）的周期和理论周期的比值（$\xi\approx1.35$）。图2(b)为不同厚度GST薄膜在硅和石英基底上激光加工制备褶皱的周期统计图，表明经过修正的预测公式能较好地拟合实验中测量的褶皱周期。同时，作为一种激光诱导热效应所生成的周期性结构，激光诱导褶皱的周期λ不受入射光波长的影响，可通过调节薄膜材料的厚度h或基底材料种类实现进一步调控，这也极大丰富了本研究提出的二维表面结构加工方法的自由度。

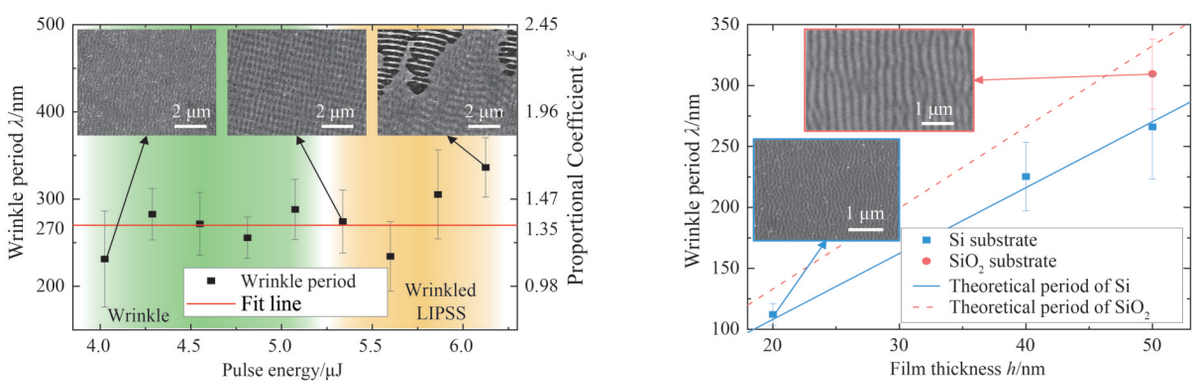

(a) Wrinkle period of 50 nm GST upon silicon substrate under laser irradiation with different pulse energies and scanning speeds of 1 mm/s

(b) Experimental and theoretical period of GST film with different thickness upon silica and silicon substrates with scanning speed of 1 mm/s

图2　激光诱导褶皱周期与加工能量、膜厚的关系

Fig. 2　Relationship between laser-induced wrinkle period and pulse energies, as well as film thicknesses

2.2　二维褶皱LIPSS的演化规律

如2.1节所述，二维褶皱LIPSS可在特定激光沉积能量和脉冲数量下产生，而进一步调控激光加工的沉积能量和脉冲数量可以使得加工结果从过度烧蚀、周期性结构生成到晶化改性的逐步演化（图3）。其中，生成的周期性结构包括单一的一维LIPSS或一维褶皱结构，以及两者共存的二维褶皱LIPSS。

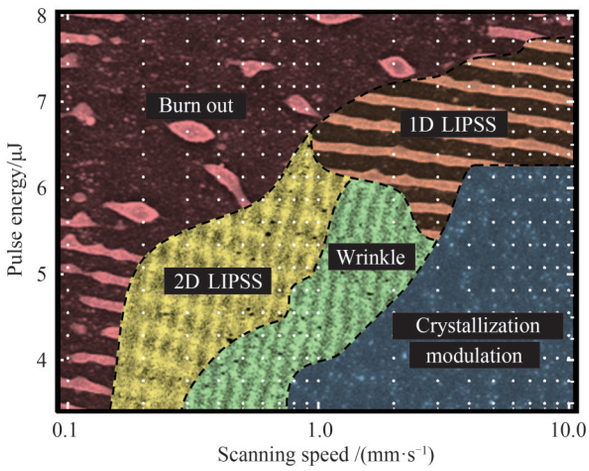

图3 脉冲重复频率为100 kHz,不同脉冲能量和扫描速度的飞秒激光加工中50 nm GST薄膜(硅基底)形成表面结构的演化坐标

Fig.3 Morphology evolution of wrinkled LIPSS on 50 nm GST thin film upon silicon through laser processing with its repetition rate of 100 kHz, different pulse energies and scanning speeds

如图3所示,相对于形成二维褶皱LIPSS的加工工况,当激光扫描速度减小时,生成LIPSS和褶皱结构等纳米结构所需的最低脉冲能量也对应减小。其中,由于褶皱结构的形成需要一定的能量沉积,而随着扫描速度的减小,单位面积内辐照的能量将随之增加,因此,褶皱结构产生所需的最小扫描速度(3 mm/s)小于LIPSS结构所需的扫描速度(>10 mm/s)。同时,在图3中,二维褶皱LIPSS和一维LIPSS以及过度烧蚀表面的划分边界不是完全分明的,在划分边界处(激光脉冲能量在5.86~6.38 μJ)二维褶皱结构中会掺杂部分的一维LIPSS结果,但在远离该临界条件的激光加工工况中,结构类型是均一的(如图2(a)中的SEM插图所示)。

上述的演化过程主要取决于激光激发表面等离激元和热累积效应的强度。如图4所示,当扫描速度为

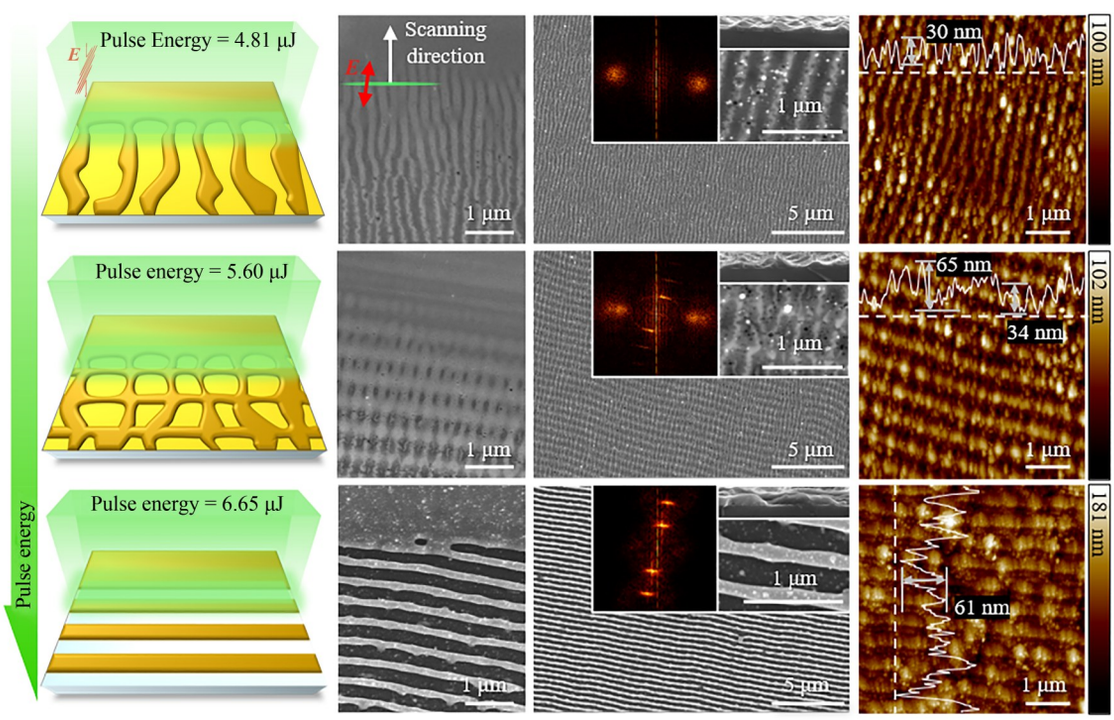

图4 在扫描速度为0.1 mm/s,不同激光能量下50 nm GST薄膜(硅基底)形成的周期性结构的示意图和SEM图,以及形成结构和其截面轮廓的SEM、二维傅里叶变换和AFM图像

Fig.4 Schematics, SEM, cross-section profile, 2D Fourier transformation, and AFM images of wrinkled LIPSS on 50 nm GST thin film upon silicon under scanning speed of 0.1 mm/s and different pulse energies

1 mm/s，使用脉冲重复频率为100 kHz的激光进行加工时，周期性结构将随着辐照激光能量的提升从褶皱结构、二维褶皱LIPSS到一维LIPSS逐步演化。在相对较低脉冲能量（4.02～5.07 μJ）下，表面等离激元的激发强度不足以引起材料烧蚀，而激光诱导热效应占主导地位，材料表面形成平行偏振方向的周期性褶皱，且随着激光扫描的持续进行，褶皱结构将进一步演化，最终材料形变所产生的褶皱深度约为30 nm。随着激光能量的增加（5.33～6.12 μJ），表面等离激元的激发强度与热累积效应诱导形成褶皱所需强度相当，在单次扫描过程中能同时形成LIPSS和褶皱结构。并由于生成机制的不同，LIPSS的均匀性略优于褶皱结构的均匀性，而LIPSS周期和深度（～410 nm，～65 nm）略大于褶皱（～288 nm，～34 nm）。当辐照激光能量相对较高（6.33～6.64 μJ）时，表面等离激元的激发强度足够，将引起材料的周期性烧蚀。而此时激光的热效应主要表现为诱导材料晶化和Marangoni效应，即在激光加工过程中，由于热效应导致GST材料发生相变并结晶生成纳米晶粒，且烧蚀过程引起的Rayleigh－Plateau不稳定将使得一维LIPSS在生成的过程中产生不稳定的无规律扰动，从而形成波纹状的光栅结构。同时，这一系列过程还将导致所生成一维LIPSS表面的不规则起伏（如图4中一维LIPSS的AFM图所示）[22]。同时，在上述不同工况下的加工过程中，由于薄膜与基底的黏附良好，明显的薄膜结构与基底剥离的现象（如图4中截面轮廓的SEM图所示）并未发生。

2.3 二维褶皱LIPSS的偏振依赖性

二维褶皱LIPSS的取向还可以通过调控入射光偏振角度实现进一步的调控。如图5中的示意插图所示，本研究中定义偏振与结构的角度为其取向与线形光源长轴的夹角。根据图5的测量统计结果可以发现LIPSS和褶皱在不同偏振角度下都几乎保持垂直。由插图中的二维傅里叶变换图像可以明显发现LIPSS的均匀性优于褶皱的结构均匀性；同时，这两种周期性结构的均匀性还与偏振角度θ相关，LIPSS在偏振角度与光源长轴平行（θ=0°）时比偏振垂直（θ～±90°）情况更均匀，而褶皱的均匀性变化趋势则相反。而这可能与表面等离激元波在不同偏振下的激发强度相关，在LIPSS生成过程中涉及平行和垂直于LIPSS的两个方向的光场增强（即光栅耦合效应和尖端光场增强效应）[14]：前者在偏振角度与光源长轴平行（θ=0°）时，使得LIPSS沿着扫描方向生长，而后者则在偏振角度与光源长轴垂直时（θ=90°）起主导作用。然而利用线光源进行加工时，偏振平行（θ=0°）加工方式生产LIPSS的均匀性通常会略微差于后者[4]。同时，在偏振垂直（θ=90°）的加工方式中，尖端光场增强效应的烧蚀占主导地位，这导致形成的褶皱结构较为不明显。此外，随着偏振角度θ的增大（－90°≤θ≤90°），两种结构的取向角度均呈现增加趋势；值得注意的是，在－45°≤θ≤45°的范围内，LIPSS的取向几乎不随θ的增大而变化，这可能与LIPSS生长过程中的尖端光场增强效应相关[14]。因此，二维褶皱LIPSS的形成存在一定的偏振敏感性，但其仍可以通过调制激光加工过程中的偏振角度进一步调控所制备二维结构取向。

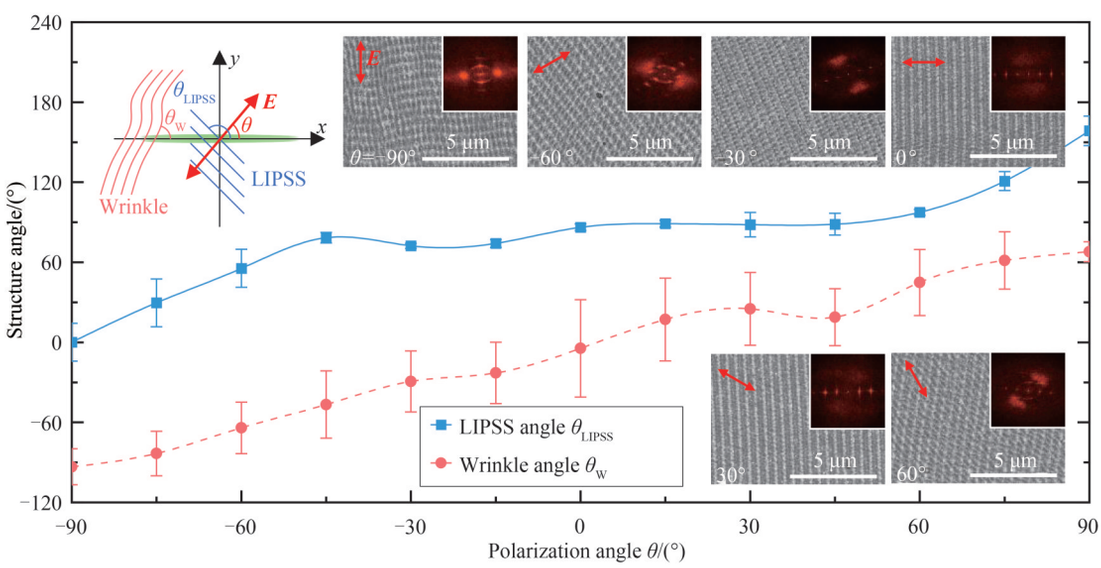

图5 不同偏振角度θ下50 nm GST薄膜（硅基底）上制备二维褶皱LIPSS的褶皱角度θ_W和LIPSS角度θ_{LIPSS}的变化趋势

Fig.5 Change curves of the angles of wrinkle angles θ_W and LIPSS θ_{LIPSS} versus polarization angle θ on 50 nm GST thin film upon silicon

3 结论

本研究提出了一种基于激光诱导周期性表面结构(LIPSS)的新型二维纳米图案化的高效激光加工方法,该方法能够在单步激光加工中实现方向、周期可控的均匀二维纳米结构的大面积制备。通过利用激光诱导的热效应和表面等离激元波的干涉,可以在激光照射过程中同时生成方向正交的褶皱和LIPSS两种周期性图案。此外,这两种结构的周期可以通过调整加工材料的膜厚(或基底材料)以及激光的波长(或入射角度)来分别实现进一步调控,而它们的方向可以通过激光偏振角度进行调节。该激光图案化方法无需掩膜、低成本,仅需通过简单的激光照射便能实现薄膜材料表面的大面积二维图案化,可为激光诱导表面结构的研究提供一种新思路。

参考文献

[1] BONSE J, HOHM S, KIRNER S V, et al. Laser-induced periodic surface structures—a scientific evergreen[J]. IEEE Journal of Selected Topics in Quantum Electronics, 2017, 23(3): 1-59.

[2] VOROBYEV A Y, GUO C. Direct femtosecond laser surface nano/microstructuring and its applications[J]. Laser & Photonics Reviews, 2013, 7(3): 385-407.

[3] BONSE J, GRÄF S. Maxwell meets Marangoni—a review of theories on laser-induced periodic surface structures[J]. Laser & Photonics Reviews, 2020, 14(10): 2000215.

[4] WANG L, CHEN Q D, CAO X W, et al. Plasmonic nano-printing: Large-area nanoscale energy deposition for efficient surface texturing[J]. Light: Science & Applications, 2017, 6(12): e17112.

[5] ZOU T, ZHAO B, XIN W, et al. High-speed femtosecond laser plasmonic lithography and reduction of graphene oxide for anisotropic photoresponse[J]. Light: Science & Applications, 2020, 9(1): 69.

[6] GENG J, YAN W, SHI L, et al. Surface plasmons interference nanogratings: wafer-scale laser direct structuring in seconds[J]. Light: Science & Applications, 2022, 11(1): 189.

[7] XU K, HUANG L, XU S. Line-shaped laser lithography for efficient fabrication of large-area subwavelength nanogratings [J]. Optica, 2023, 10(1): 97.

[8] HUANG M, ZHAO F, CHENG Y, et al. Origin of laser-induced near-subwavelength ripples: interference between surface plasmons and incident laser[J]. ACS Nano, 2009, 3(12): 4062-4070.

[9] ZHENG J, HUANG J, XU S. Multiscale micro-/nanostructures on single crystalline SiC fabricated by hybridly polarized femtosecond laser[J]. Optics and Lasers in Engineering, 2020, 127: 105940.

[10] DURBACH S, KRAUSS F T, HOFFMANN M, et al. Laser-driven one- and two-dimensional subwavelength periodic patterning of thin films made of a metal-organic MoS_2 precursor[J]. ACS Nano, 2022, 16(7): 10412-10421.

[11] MASTELLONE M, BELLUCCI A, GIROLAMI M, et al. Deep-subwavelength 2D periodic surface nanostructures on diamond by double-pulse femtosecond laser irradiation[J]. Nano Letters, 2021, 21(10): 4477-4483.

[12] ZHENG X, ZHAO B, YANG J, et al. Noncollinear excitation of surface plasmons for triangular structure formation on Cr surfaces by femtosecond lasers[J]. Applied Surface Science, 2020, 507(November 2019): 144932.

[13] ÖKTEM B, PAVLOV I, ILDAY S, et al. Nonlinear laser lithography for indefinitely large-area nanostructuring with femtosecond pulses[J]. Nature Photonics, 2013, 7(11): 897-901.

[14] HUANG J X, XU K, XU S L, et al. Self-aligned laser-induced periodic surface structures for large-area controllable nanopatterning[J]. Laser & Photonics Reviews, 2022, 16(5): 2200093.

[15] HUANG J, XU K, HU J, et al. Self-aligned plasmonic lithography for maskless fabrication of large-area long-range ordered 2D nanostructures[J]. Nano Letters, 2022, 22(15): 6223-6228.

[16] DOSTOVALOV A, BRONNIKOV K, KOROLKOV V, et al. Hierarchical anti-reflective laser-induced periodic surface structures (LIPSSs) on amorphous Si films for sensing applications[J]. Nanoscale, 2020, 12(25): 13431-13441.

[17] HUANG J, WANG X, MIZUTANI M, et al. Generation mechanisms of laser-induced periodic nanostructures on surfaces of microgrooves[J]. Optics and Laser Technology, 2023, 160: 109056.

[18] DESTOUCHES N, SHARMA N, VANGHELUWE M, et al. Laser-empowered random metasurfaces for white light printed image multiplexing[J]. Advanced Functional Materials, 2021: 2010430.

[19] MA H, DALLOZ N, HABRARD A, et al. Predicting laser-induced colors of random plasmonic metasurfaces and optimizing image multiplexing using deep learning[J]. ACS Nano, 2022, 16(6): 9410-9419.

[20] DALLOZ N, LE V D, HEBERT M, et al. Anti-counterfeiting white light printed image multiplexing by fast nanosecond laser processing[J]. Advanced Materials, 2022, 34(2): 2104054.

[21] MAKAROV S V, TSYPKIN A N, VOYTOVA T A, et al. Self-adjusted all-dielectric metasurfaces for deep ultraviolet femtosecond pulse generation[J]. Nanoscale, 2016, 8(41): 17809-17814.

[22] YUAN D, HUANG J, LI J, et al. Laser constructing short-range disordered metagratings for visible near-infrared polarization-independent absorption[J]. Advanced Optical Materials, 2023: 2202585.
[23] LIU N, SUN Q, YANG Z, et al. Wrinkled interfaces: taking advantage of anisotropic wrinkling to periodically pattern polymer surfaces[J]. Advanced Science, 2023: 2207210.
[24] GROENEWOLD J. Wrinkling of plates coupled with soft elastic media[J]. Physica A: Statistical Mechanics and its Applications, 2001, 298(1-2): 32-45.
[25] LEE J H, RO H W, HUANG R, et al. Anisotropic, hierarchical surface patterns via surface wrinkling of nanopatterned polymer films[J]. Nano Letters, 2012, 12(11): 5995-5999.
[26] FILLOT F, SABBIONE C. Nanoscale mechanics of thermally crystallized GST thin film by in situ X-ray diffraction [J]. Journal of Applied Physics, 2020, 128(23): 235107.
[27] CALLISTER W D JR, RETHWISCH D G. Fundamentals of materials science and engineering [M]. 5th ed. Wiley, 2018: 858-863.

Laser-induced Two-dimensional Surface Nanopatterning on Film Materials (Invited)

HUANG Jiaxu, LI Jun, QIU Pei, XU Shaolin
(*Department of Mechanical and Energy Engineering, Southern University of Science and Technology, Shenzhen* 518055, *China*)

Abstract: Laser-Induced Periodic Surface Structures (LIPSS) have been extensively studied as grating structures that form beyond the diffraction limit under laser irradiation over a large area. However, most LIPSS are essentially one-dimensional (1D) gratings, and this limited range of structural types in LIPSS hampers their widespread applications. To overcome this challenge, our study proposes a novel maskless two-dimensional (2D) laser nanopatterning method that combines the utilization of laser-induced thermal deformation effects and laser-Surface-Plasmon-Polaritons (SPPs) interference. By harnessing these two effects simultaneously, we can create two distinct periodic structures, namely wrinkles and LIPSS, in orthogonal directions. This innovative approach enables the generation of 2D wrinkled LIPSS on thin-film materials through a single-step laser irradiation process. Moreover, we have made significant advancements in the spatial modulation of the irradiated femtosecond laser, achieving a line shape with a length of 8 mm and a width of 7.78 μm. This spatial modulation facilitates efficient nanopatterning of these 2D LIPSS on a millimeter scale within seconds. These breakthroughs greatly expand the range of achievable structural types with LIPSS, making them more suitable for mass micro/nano fabrication. Our investigation focuses on the formation of wrinkles and LIPSS on $Ge_2Sb_2Te_5$ (GST) thin-film materials, with an emphasis on laser-induced thermal accumulation, thermal deformation, and laser-SPPs interference. During the laser-induced thermal deformation, wrinkles spontaneously generate with a period of approximately 270 nm on a 50-nm-thick GST film over a silicon substrate. Importantly, these wrinkles maintain their stability in terms of their periods under laser irradiation with varying laser pulse energies. Furthermore, their periods can also be accurately controlled and predicted through a thermal deformation model, which has been validated on GST thin films with different thicknesses and substrate materials. Similarly, another periodic structure, namely LIPSS, can also spontaneously form due to the periodic ablation caused by laser-SPPs interference. The periods of LIPSS, measuring around 410 nm on the same 50-nm-thick GST film, can be modulated by adjusting parameters such as laser wavelength or incident angle. This independent modulation capability allows precise control over the periods of 2D wrinkled LIPSS in both orthogonal directions. Furthermore, we explore the morphological evolution of 2D wrinkled LIPSS and observe a gradual transition from excessive ablation and periodic structure generation to simple crystallization modification as the scanning speed increases or the laser pulse energy decreases. By manipulating the excitation intensity of laser-induced thermal effects and laser-SPPs interference through increasing the laser pulse energy under a fixed scanning speed, we can freely transform the generated periodic structures from wrinkled structures and 2D wrinkled LIPSS to 1D LIPSS. It is worth noting that the height of LIPSS can exceed 65 nm, while the corresponding wrinkle heights typically reach around

34 nm. Additionally, the orientation of 2D wrinkled LIPSS can be controlled by adjusting the polarization angle of the incident laser, adding another parameter to manipulate these structures. Moreover, we have discovered that 2D wrinkled LIPSS formed under different laser polarizations exhibit varying levels of uniformity. Comparatively, LIPSS display superior uniformity when compared to wrinkles, with their orientation being influenced by the polarization angle of the irradiated laser. The laser nanopatterning method proposed in this study demonstrates the immense potential for enhancing the diversity and expanding the applications of LIPSS. It not only overcomes the limitations associated with the monotonous structural type of 1D gratings in LIPSS but also offers a versatile means to engineer and customize the properties of thin-film materials. The increased range of structural possibilities and control over orientations pave the way for a great variety of applications, including surface modification, bionic structural coloration, high-precision detection, photonics, and optoelectronics. The findings presented in this study contribute to advancing laser nanopatterning techniques and provide valuable insights for future research in laser nanofabrication, a rapidly evolving field.

Key words: Ultrafast laser; Laser-Induced Periodic Surface Structures (LIPSS); Laser-induced wrinkle; Thin film materials; 2D nanostructures; Femtosecond laser

OCIS Codes: 220.4241; 310.6628; 320.7090

Foundation item: Shenzhen Science and Technology Programs (Nos. JCYJ20220818100408019, JSGG20210802154007021, KQTD20170810110250357)